Silylation Efficiency of Chorosilanes, Alkoxysilanes, and Monosilazanes on Periodic Mesoporous Silica

ARTICLE *in* THE JOURNAL OF PHYSICAL CHEMISTRY C · DECEMBER 2010

Impact Factor: 4.77 · DOI: 10.1021/jp107749g

3 AUTHORS, INCLUDING:

Yucang Liang
University of Tuebingen
86 PUBLICATIONS **2,148** CITATIONS

SEE PROFILE

Silylation Efficiency of Chorosilanes, Alkoxysilanes, and Monosilazanes on Periodic Mesoporous Silica

Thomas Deschner,[†] Yucang Liang,[‡] and Reiner Anwander*[,†,‡]

Kjemisk Institutt, Universitetet i Bergen, Allégaten 41, 5007 Bergen, Norway, and Institut für Anorganische Chemie, Eberhard Karls Universität Tübingen, Auf der Morgenstelle 18, 72076 Tübingen, Germany

Received: August 16, 2010; Revised Manuscript Received: October 14, 2010

Because of their large surface area and distinct pore architecture, periodic mesoporous silica (PMS) are predisposed to study the reactivity of surface silanol groups. Surface silylation involving the formation of thermodynamically stable $O-SiR_3$ moieties is a powerful and probably the most prominent postsynthesis functionalization method of oxidic support materials. This study will assess the reactivity/silylation behavior of similarly sized dimethyloctylsilazane ($Me_2NSiMe_2(C_8H_{17})$), dimethyloctylchlorosilane ($ClSiMe_2(C_8H_{17})$), and octyltriethoxysilane ($(EtO)_3Si(C_8H_{17})$), toward periodic mesoporous silica MCM-41 (BET surface a_s = 1060 m^2/g, pore volume V_p = 1.14 cm^3/g, pore diameter d_p = 4.0 nm, silanol population = 3.47 mmol/g) and SBA-1 (a_s = 1260 m^2/g, V_p = 0.73 cm^3/g, D_{me} = 4.5 nm, silanol population = 4.45 mmol/g). A medium-long aliphatic tail (C_8) was chosen to ensure a reliable elemental (carbon) analysis and to study any size-selective behavior of cagelike SBA-1. For channel-like MCM-41, the obtained hybrid materials reveal a superior silylation efficiency (SE) of the monosilazane reagent compared to the chloro- and ethoxysilanes (SE = 81% versus 67% versus 22%, use of excess of silylating reagent), the latter two reagents requiring either elevated temperature (125 °C) or stoichiometric amounts of a base (NEt_3). For cagelike SBA-1, site-specific reactivity of the monosilazane reagent at the outer surface and pore openings was observed, finally resulting in pore blockage. Even under harsher reaction conditions, the chloro- and ethoxysilanes gave a more random surface silylation, however with lower SE values (SE = 76% versus 62% versus 32%; use of excess of silylating reagent). All materials were characterized by FTIR spectroscopy, nitrogen physisorption, elemental analysis, and transmission electron microscopy.

Introduction

Surface silylation involving the formation of thermodynamically stable $O-SiR_3$ moieties is a powerful and probably the most prominent postsynthesis functionalization method of oxidic support materials.[1−4] Not surprisingly, postsynthesis silylation has developed into a popular approach for tailoring the surface morphology and reactivity of periodic mesoporous silicas (PMSs).[5−7] As a rule, applications of channel- (e.g., M41S family)[8] and cagelike PMS materials (e.g., SBA-1,[9,10] SBA-2,[9,10] SBA-16,[11,12] and KIT-5[13]) in adsorption processes,[14−16] chromatography,[7,17,18] as sensors,[7,19−21] in gas storage or catalysis[7,22−32] imply specially designed functionalizations of the purely inorganic host. In addition to co-condensation (one-pot) procedures, employing mixtures of (functionalized) alkoxysilanes,[21,33−40] and PMO (periodic mesoporous organosilica) reaction protocols,[41−45] the surface modification of PMS materials (grafting) is a very efficient method to fabricate such porous (metal)organic−inorganic hybrid materials.[5,6,24,28,30,32,46,47] Whereas all these (silylation) methods predominantly aim at tuning the hydrophobicity of the respective materials, enhanced thermal stability can occur as a beneficial side effect.[16,18,48−50]

General advantages of postsynthesis silylation approaches are that (a) the ideally long-range ordered parent PMS material can easily be obtained free of surfactant (template) by a simple calcination step (more demanding extraction processes are unnecessary), (b) silylation does not affect the long-range ordering of the PMS material, (c) a (high) loading of the functional groups can be controlled via thermal pretreatment of the parent PMS material, (d) anhydrous reaction conditions allow for the use of highly reactive reagents, and (e) the surface reactivity can be easily tuned by the availability of different silylating reagents. The latter comprise not only chlorosilanes,[5,14,16,21,50−61] alkoxysilanes,[5,62−66] and silazanes[24,25,27,46,47,60,61,67−73] (also called silylamines), which represent the most important classes of silylating reagants but also more sophisticated silylating reagents like for example *N*,O-bis(trimethylsilyl)trifluoro acetamide, $[CF_3COSiMe_3]=NSiMe_3$[31] and allylsilanes[74] (Scheme 1).

The grafting rate depends on the reactivity of the silylating reagent, diffusion limitations, and steric factors. Because of their limited reactivity toward silanol groups, chlorosilanes $ClSiR_3$ and alkoxysilanes $(R'O)_xSiR_y$ usually require more drastic reaction conditions − either elevated temperatures and/or the prescence of catalytic (e.g., H_2O) or stoichiometric (e.g., pyridine) amounts of additives. Concomitantly, multifunctional surface reactions occur, producing (undesired and difficult-to-separate) byproducts such as alcohols and alkylammonium halides. The silylation reactivity of silazanes decreases in the order monosilazanes R'_2NSiR_3 > disilazanes $HN(SiR_3)_2$ > trisilazanes $N(SiR_3)_3$.[61] Overall, silazanes feature superior silylating reagents as revealed by (i) mild reaction conditions, (ii) relatively slow surface reaction (in the case of di- and trisilazanes), (iii) a monofunctional surface reaction, (iv) favorable atom economy, and (v) ease of thermal desorption of the excess silylamine and the byproduct ammonia. Further, a rich pool of

* To whom correspondence should be addressed. E-mail: Reiner.Anwander@uni-tuebingen.de. Phone: +4970712972069. Fax: +497071292436.
† Universitetet i Bergen.
‡ Eberhard Karls Universität Tübingen.

10.1021/jp107749g
Published on Web 12/08/2010

SCHEME 1: Methods of Surface Silylation

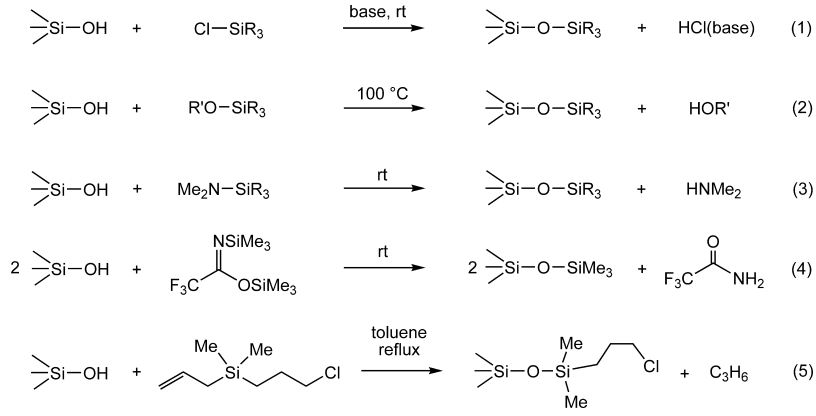

silazanes is commercially available and new derivatives are readily synthesized.[6,24,61,67]

We are particularly interested in cagelike materials like SBA-1, SBA-2, SBA-16, and KIT-5 because their 3D structure and pore connectivity provide a unique environment for shape and size selective catalysis:[30,75−77] mesosized, spherical, or ellipsoidal supercages are three-dimensionally linked via smaller channels or windows. Recently, we described a method for the rational design of size-selective catalysts on the basis of cagelike mesopourous silicas of the SBA-*n* family, featuring surface silylation as a crucial functionalization step and SBA-1 as the most promising material for this application.[30] Herein, we present a silylation study of channel-like MCM-41 and cagelike SBA-1 assessing for the first time the comparative performance and efficiency of the most important classes of silylating reagents: chlorosilanes, alkoxysilanes, and silylamines.

Experimental Section

General Materials. The silylation reactions were performed under dry argon using glovebox techniques (MB Braun MB150B-G-II; <1 ppm O_2, <1 ppm H_2O). Hexane and toluene were purified by using Grubbs columns (MBraun SPS, solvent purification system) and stored in a glovebox. Dimethyloctylchlorosilane and octyltriethoxysilane were purchased from Aldrich. 1,1,3,3-Tetramethyldisilazane was obtained from ABCR and used as received. Triethylamine was acquired from Fluka. Dimethyloctylchlorosilane, octyltriethoxysilane, and triethylamine were distilled and degassed prior to use. Dimethyloctylsilazane was synthesized from equimolar amounts of dimethyloctylchlorosilane and dimethyllithium amide in a mixture of *n*-hexane and THF at ambient temperature.[30] PMS materials MCM-41 (**1**) and SBA-1 (**2**, **3**) were synthesized according to slightly modified literature procedures.[57,61,72,78−80] Detailed syntheses are described in the Supporting Information.

General Synthesis of the Hybrid Materials. The PMS materials were suspended in ca. 5−10 mL dry solvent (hexane or toluene). To this suspension, the respective amounts of silylation reagent and/or base in ca. 5 mL of solvent were added. For better comparability, the reaction mixtures were stirred for 18 h either at ambient temperature or under reflux conditions (125 °C). The silylated materials were washed three times with hexane and centrifuged after each washing step. The remaining solvent was removed under vacuum at ambient temperature and by degassing for 3 h at 10^{-3} Torr to yield the resulting hybrid materials. Prior to the degas step, the materials derived from the chlorosilanes were additionally treated for 4 h at 100 °C under high vacuum to ensure a successful removal of the ammonium halide (for detailed synthesis procedures see Supporting Information).

Characterization. Powder X-ray diffraction (PXRD) patterns were recorded on a Bruker D8 ADVANCE instrument in the step/scan mode (step width = 0.00825, accumulation time = 2 s/step, range (2θ) = 0.50−10.00°) using monochromatic CuKα radiation (λ = 1.5418 Å). IR spectra of the parent and silylated materials were recorded on a Nicolet Impact 410 FTIR spectrometer using Nujol mulls sandwiched between CsI plates. DRIFT spectra were reorded on a Nicolet 6700 FTIR spectrometer using dried KBr powder and KBr windows. Transmission electron micrographs (TEM) were obtained using a JEOL JEM2100 operated at 160 kV. For TEM observations, the materials were crushed and suspended in ethanol (99.9%) using ultrasonic treatment. A drop of this suspension was loaded onto a holey carbon film on an Agar grid with a square 400 mesh (copper; 3.05 mm). Scanning electron microscopy (SEM) images were recorded on a JEOL JSM-5900LV microscope equipped with an EDX system and operated at an accelerating voltage of 15 kV. All SEM images reported here are representative of the corresponding materials. Nitrogen adsorption/desorption isotherms were measured with an ASAP 2020 volumetric adsorption apparatus (Micromeritics) at 77.4 K for relative pressures from 1×10^{-2} to 0.99 ($a_m(N_2, 77\ K) = 0.162\ nm^2$). The BET specific surface area was obtained from the nitrogen adsorption data in the relative pressure range from 0.1 to 0.15 for SBA-1 materials and from 0.1 to 0.2 for MCM-41 materials.[81,82] The pore size distributions were calculated using the Barrett−Joyner−Halenda (BJH) method as a routine method.[83] The BJH method systematically underestimates the effective pore diameter of hexagonal and cagelike materials.[67] Therefore the cage diameters of the parent and hybrid SBA-1 materials were calculated according to the model of spherical cavities using equation $D_{me} = a(6\epsilon_{me}/(\pi\upsilon))^{1/3}$, which has been proposed by Ravikovitch and Neimark.[84] D_{me} is the diameter of the cavities within the unit cell of length a (a and c), ϵ_{me} is the volume fraction of a regular cavity, $\epsilon_{me} = \rho_v V_{me}/(1 + \rho_v V_{me})$, where $\rho_v = 2.2\ g\ cm^{-3}$ is the estimated silica wall density and υ is the number of cavities per unit cell (for $Pm\bar{3}n$, $\upsilon = 8$). Additionally, the pore diameters of the parent and silylated MCM-41 materials were determined by a method described by Kruk, Jaroniec, and Sayari (KJS-method; see Supporting Information).[85,86] Elemental analyses were performed on an Elementar VarioEL III instrument. The surface silanol population was obtained from the surface coverage (SiR_3) of silylated samples activated at 250 °C/10^{-2} Torr for 2.5 h as described previously.[47]

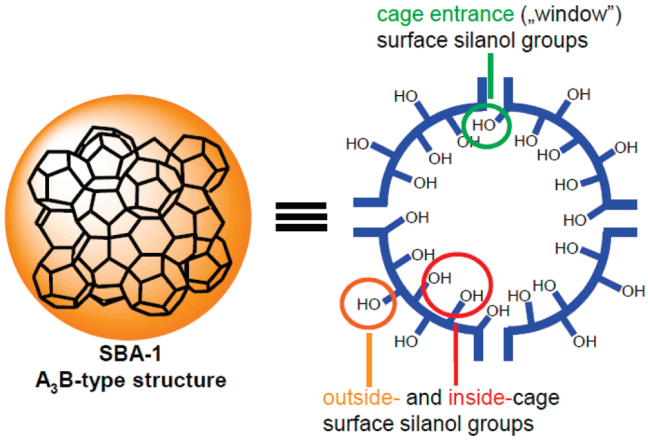

Figure 1. Simple model of cagelike SBA-1 showing three different silanol environments.

Results and Discussion

Hexagonal MCM-41 (space group *p6mm*) and cubic SBA-1 ($Pm\bar{3}n$)[57,79,80,87] PMSs were selected to study any distinct silylation behavior associated with a channel- or a cagelike pore configuration. Dimethyloctylsilazane ($Me_2NSiMe_2(C_8H_{17})$, **A**), dimethyloctylchlorosilane ($ClSiMe_2(C_8H_{17})$, **B**), and octyltriethoxysilane ($(EtO)_3Si(C_8H_{17})$, **C**), with a medium-long aliphatic tail (C_8) were chosen as silylating reagents to ensure a reliable elemental (carbon) analysis and to study any size-selective behavior of cagelike SBA-1. All materials were characterized via infrared spectroscopy, nitrogen physisorption, and elemental analysis.

In contrast to the 1D cylindrical channels of MCM-41, SBA-1 possesses a A_3B-structure, which consists of two differently sized cages, with cage A being marginally larger than cage B (ratio: 1.1). The cage diameters strongly depend on the synthesis conditions, but as a rule of thumb, cage B is spherical with a pore diameter of around 33 Å, whereas cage A possesses an ellipsoidal shape and a pore diameter in the 40 Å-region. On the basis of electron diffraction experiments by Sakamoto et al.,[88] the windows connecting two A-cages show sizes in the region of 15 × 22 Å. Windows between A-and B-cages are supposed to be around 2 Å in diameter. Calculations by Anderson et al.[89] show that the maximum diameter of the windows is 13 Å. It is therefore not possible to directly assess the chemical accessibility of the SBA-1 pore system via these methods. A simplified model for SBA-1 providing us with the most important features of this material is shown in Figure 1. Roughly, SBA-1 displays silanol groups in three different environments: inside-cage, cage-window, and outside-cage. Hence, any postsynthesis treatment selectively addressing these silanol groups becomes a challenging task. More precisely, SBA-1-based (reactant) size-selective catalysis would require a selective modification of the outer surface and tuning of the pore openings in such a manner, that the catalytic species, which should then be located exclusively inside the cages, is accessible only for the smaller-sized molecules out of a mixture of differently sized reactants.[30]

Surface Silylation of MCM-41. First, the SiOH population (accessible OH groups) of MCM-41 material **1**, showing a pore diameter of 4.0 nm according to the BJH adsorption branch (4.9 nm according to the KJS-method,[85] for more information see Table S1 of the Supporting Information), a BET surface of 1060 m^2/g and a pore volume of 1.14 cm^3/g, was determined as 3.47 mmol/g by functionalization with the small disilazane reagent $HN(SiHMe_2)_2$ (material **1a**).[47] Note that the BJH method underestimates the true pore diameter, whereas the KJS-method quite accurately reproduces the true pore diameter of hexagonal materials (in the following, the value obtained via the KJS-method is given in parentheses). When targeting the silylation of one-third of the accessible SiOH groups, silazane **A** and chlorosilane **B** (triethylamine used as a base) gave materials **1b** and **1c**, both exhibiting a silylation efficiency (SE) of around 90% (Table 1). Even though harsher conditions were applied when reacting the ethoxysilane **C** with the MCM-41 material at 125 °C in toluene, the resulting material **1d** showed only a SE of 24%. This different SE is also reflected by the nitrogen physisorption analysis, revealing a higher BET surface area and pore volume for the latter material **1d** (Figure 2).

Similar trends were observed by using excess of the silylating reagent except that now silazane reagent **A** (**1e**: SE = 81%) seems to outperform even chlorosilane **B** (**1f**: SE = 67%). As expected, the degree of silylation is now considerably higher as documented by higher measured carbon values. Not surprisingly, ethoxysilane **C** shows the worst performance (**1g**: SE = 22%). The silazane and chlorosilane silylations decreased the pore volume drastically to approximately one-third of the initial one, that is, to 0.35 (**1e**) and 0.46 cm^3/g (**1f**) respectively, whereas for the ethoxysilyl-functionalized material **1g** it was still twice as high (0.78 cm^3/g). As a general trend, loading of the surface with silyl groups does not only decrease the pore

TABLE 1: Analytical Data, Surface Area, Pore Volume, and Pore Diameter of Parent and Silylated MCM-41 Materials

sample	ratio of silylating reagent and SiOH population[a]	silylating reagent	a_s [m^2/g][b]	$d_{p,ads}$ [nm][c]	pore diameter (w_d, w_{mod}) [nm][d]	V_p [cm^3/g][e]	C [wt%][f]	SE [%][g]
1			1060	4.0	4.9	1.14		
1a	excess	$HN(SiHMe_2)_2$	740	3.3	4.3	0.73	6.94	100
1b	$^1/_3$	$C_8H_{17}SiMe_2NMe_2$	730	3.1	4.2	0.70	11.66	90
1c	$^1/_3$	$C_8H_{17}SiMe_2Cl$[h]	660	3.0	4.0	0.61	14.34	92
1d	$^1/_3$	$C_8H_{17}Si(OEt)_3$[i]	840	3.8	4.4	0.87	5.08	24
1e	1.15	$C_8H_{17}SiMe_2NMe_2$	440	2.5	3.3	0.35	22.75	81
1f	1.15	$C_8H_{17}SiMe_2Cl$[h]	530	2.7	3.7	0.46	20.08	67
1g	1.2	$C_8H_{17}Si(OEt)_3$[i]	770	3.6	4.3	0.78	7.92	22

[a] SiOH population calculated from the corrected carbon value of the dimethylsilylated samples. [b] Specific BET surface area. [c] Pore diameter according to the maximum of the BJH pore size distribution calculated from the adsorption branch; all samples were pretreated at 250 °C (parent materials) and 100 °C (silylated samples) in vacuo until the pressure was $<10^{-3}$ Torr. [d] Assessed from the KJS-method (Supporting Information).[85,86] [e] Pore volume determined at the relative pressure $p/p_0 = 0.975$. [f] Elemental analysis obtained after treatment at 100 °C in vacuo ($<10^{-3}$ Torr). [g] The silylation efficiency SE was determined by the molar ratio of the grafted species divided by the maximum amount of silanol groups that could be grafted using $HN(SiHMe_2)_2$ (based on the assumption that the corrected carbon-value of the elemental analysis divided by the amount of carbon atoms corresponds to the molar amount of the grafted species). [h] Reaction conditions: NEt_3 as a base, stirring at ambient temperature, solvent: *n*-hexane. [i] Reaction conditions: stirring at 125 °C, solvent: toluene.

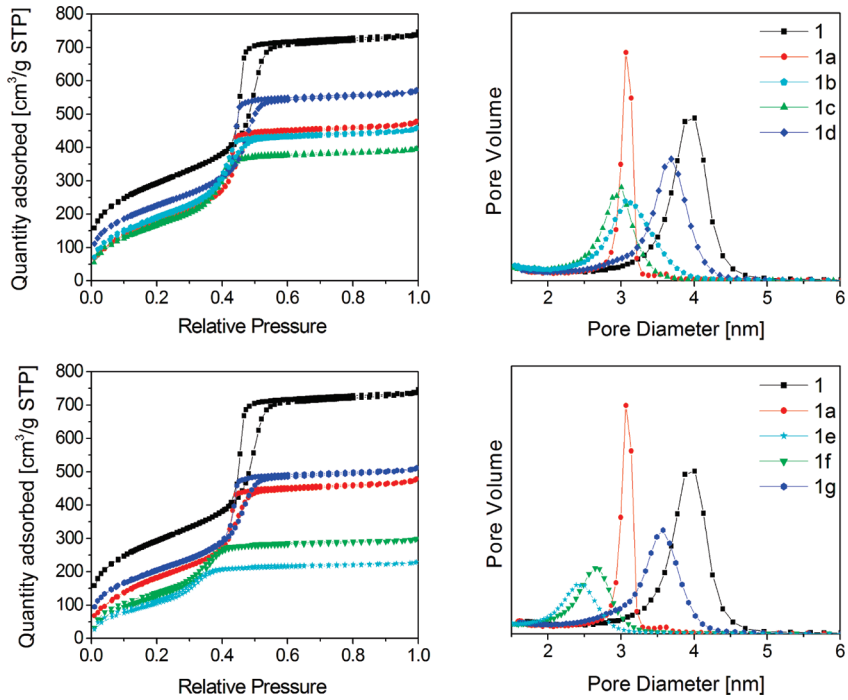

Figure 2. Nitrogen physisorption isotherms and respective pore size distributions of the surface-silylated MCM-41 materials under study: top, maximum $^1/_3$ of the MCM-41 silanol groups silylated; bottom, excess of silylating reagent has been used.

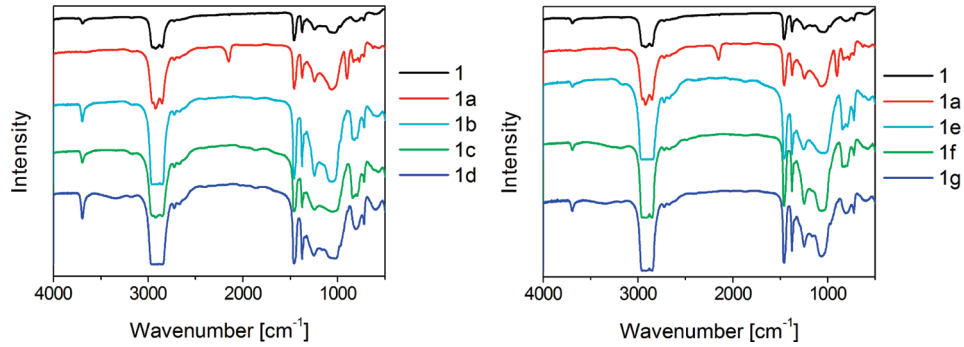

Figure 3. Infrared spectra of the surface-silylated MCM-41 materials under study: left, maximum $^1/_3$ of the MCM-41 silanol groups silylated; right, excess of silylating reagent has been used.

diameter and the pore volume, but also the BET surface area with increasing degree of silylation. Correspondingly, maximum decrease of the pore diameter was observed for material **1e** (4.0 → 2.5 nm, according to the BJH-method; 4.9 → 3.3 nm, according to KJS-method). All silylated MCM-41 materials except **1e** and **1f** show a typical *type IV* isotherm with a *H2* hysteresis loop in the region of relative pressure of around 0.4−0.6 (Figure 2). Materials **1e** and **1f** exhibit a *type IV* isotherm without any hysteresis loop. All C_8-silylated MCM-41 materials still show nonreacted silanol groups as evidenced by the IR vibration at 3695 cm^{-1} (Figure 3), which means, that even with excess of silazane reagent **A** not all silanol groups are consumed/are accessible, under the prevailing reaction conditions.

The general low reactivity of alkoxysilanes in dry solvents is well-documented[6,90] and the higher SE of monosilazane **A** compared to chlorosilane **B** can be rationalized on the kinetic control of the formation of the intermediate surface species as shown in Figure 4. The surface reaction of the chlorosilane **B** requires further activation of the surface silanol with the base NEt_3 implying enhanced steric congestion.

The overall incomplete surface silylation even for the most reactive reagent **A** is most likely due to diffusion restrictions

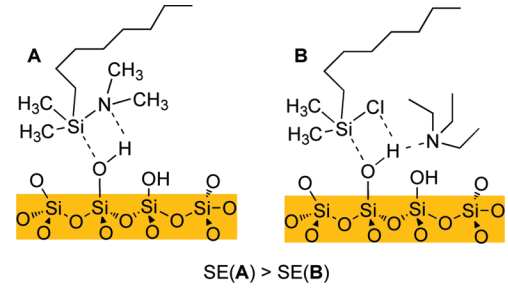

Figure 4. Kinetic control of surface silylation. Proposed intermediates of the reaction of monosilazane (**A**) and chlorosilane (**B**) reagents with silanol groups.

and limited accessibility of the remaining surface silanol groups of partly C_8-silylated materials. This is in accordance with previous work by (a) Antochshuk et al., who reasoned that bending of the C_8-alkyl chain shields neighboring silanol groups from reacting with another molecule of silazane[53] and (b) us, showing that the reaction of the corresponding disilazane reagent $HN[SiMe_2(C_8H_{17})]_2$ with a 2.8 nm pore-sized MCM-41 produced a similar SE of 76%.[47] In addition, it has been reported, that pores of diameter of 2.4 nm can be blocked by a C_8-spacer,[91] but since the 4.0 nm (4.9 nm) pore diameter of MCM-41

TABLE 2: Analytical Data, Surface Area, Pore Volume, and Pore Diameter of Parent and Silylated SBA-1 Materials

sample	ratio of silylating reagent and SiOH population[a]	silylating reagent	a_s [m^2/g][b]	d_p [nm][c]	D_{me} [nm][d]	V_p [cm/g][e]	C [wt%][f]	SE [%][g]
2			1260	2.3	4.5	0.73		
2a	excess	$HN(SiHMe_2)_2$	550	1.7	3.6	0.22	8.49	100
2b	$^1/_3$	$C_8H_{17}SiMe_2NMe_2$	630	<1.6	3.7	0.26	13.62	88
2c	$^1/_3$	$C_8H_{17}SiMe_2Cl$[h]	1190	2.2	4.4	0.64	4.47	27
2d	$^1/_3$	$C_8H_{17}Si(OEt)_3$[h]	1010	2.2	4.2	0.51	7.48	46
3			1360	2.5	4.5	0.88		
3a	excess	$HN(SiHMe_2)_2$	930	2.2	4.1	0.49	7.36	100
3b	1.05	$C_8H_{17}SiMe_2NMe_2$	30	n.d.	1.6	0.01	22.86	76
3c	1.50	$C_8H_{17}SiMe_2Cl$[h]	1080	2.5	4.3	0.62	7.65	19
3d	1.10	$C_8H_{17}SiMe_2Cl$[i]	470	2.0	3.5	0.21	19.98	62
3e	1.50	$C_8H_{17}Si(OEt)_3$[h]	870	2.1	4.1	0.48	12.27	32

[a] SiOH population calculated from the corrected carbon value of the dimethylsilylated samples. [b] Specific BET surface area. [c] Pore diameter according to the maximum of the BJH pore size distribution calculated from the adsorption branch; all samples were pretreated at 250 °C (parent materials) and 100 °C (silylated samples) in vacuo until the pressure was $<10^{-3}$ Torr. [d] Cage diameter according to the model of spherical cavities as proposed by Ravikovitch and Neimark.[84] [e] Pore volume determined at the relative pressure $p/p_0 = 0.975$. [f] Elemental analysis obtained after treatment at 100 °C in vacuo ($<10^{-3}$ Torr). [g] The silylation efficiency SE was determined by the molar ratio of the grafted species divided by the maximum amount of silanol groups that could be grafted using $HN(SiHMe_2)_2$ (based on the assumption that the corrected carbon-value of the elemental analysis divided by the amount of carbon atoms present the molar amount of the grafted species). [h] Reaction conditions: stirring at 125 °C, solvent: toluene. [i] Reaction conditions: using NEt_3 as a base, stirring at room temperature, solvent: *n*-hexane.

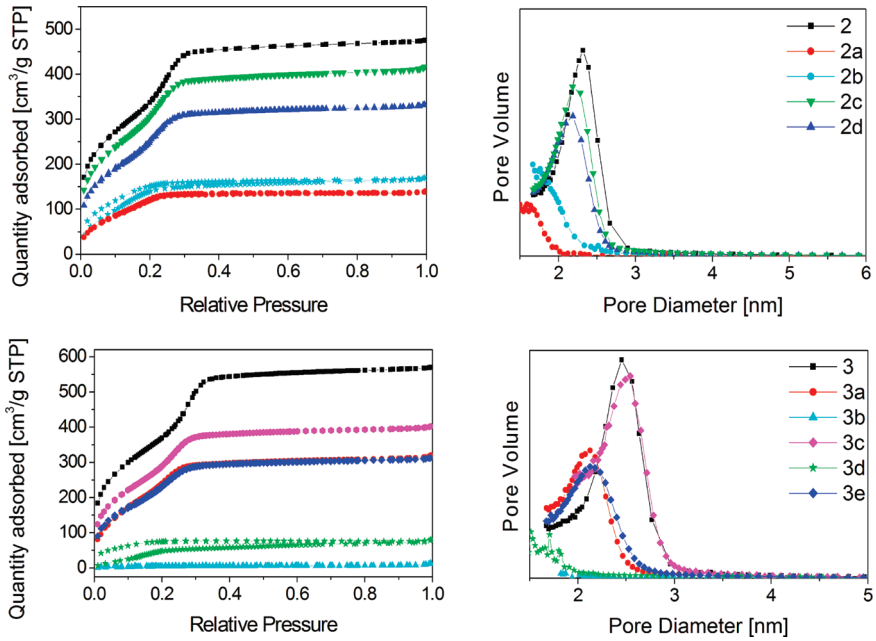

Figure 5. Nitrogen physisorption isotherms and respective pore size distributions of the surface-silylated SBA-1 materials under study: top, maximum $^1/_3$ of the SBA-1 silanol groups silylated; bottom, excess of silylating reagent has been used.

material **1** is significantly larger, it is unlikely that the incomplete silylation of materials **1e** and **1f** is due to pore blockage.

Surface Silylation of SBA-1. Two routine SBA-1 materials (**2** and **3**) were used to evaluate any size-limiting implications of the cage windows for the silylation performance. Pore-enlarged SBA-1 materials **4** and **5** implied similar surface reactivity of the silylating reagents **A**, **B**, and **C** and the results herefrom are therefore only shown in the Supporting Information. Material **2** ($a_s = 1260$ m^2/g, $V_p = 0.73$ cm^3/g, $D_{me} = 4.5$ nm, 4.45 mmol SiOH/g) was used to examine surface silylations with the ratio of the silylating reagents and silanol population set to $^1/_3$. Note that D_{me} represents the cage diameter and not any pore opening. Silylation with monosilazane **A** yielding material **2b** was almost complete (SE = 88%), whereas chorosilane **B** and ethoxysilane **C** gave poor efficiencies of 27% (**2c**) and 46% (**2d**), respectively (Table 2). Note that the chlorosilane silylation was now performed in the absence of the base NEt_3.

For material **2b**, only 30% of the original pore volume was left although only one-third of the silanol groups were consumed. The nitrogen physisorption measurements revealed a *type I* isotherm for the highly silylated material **2b**, whereas materials **2c** and **2d** display typical features of *type IV* isotherms (Figure 5). The IR spectra of all silylated materials **2b-d** show nonreacted silanol groups (Figure 6).

These features indicate already that silazane **A** reacts preferentially with the silanol groups located at the outer surface and the pore openings (windows) of the cubic material. This could be corroborated further by reacting SBA-1 material **3** ($a_s = 1360$ m^2/g, $V_p = 0.88$ cm^3/g, $D_{me} = 4.5$ nm, 3.73 mmol SiOH/g) with excess of the silylating reagents. Clearly, pore blockage occurred for monosilazane **A**, being caused by rapid consumption of all silanol groups located at the outer surface and at the outer cages/cage windows of the SBA-1 primary particles. Considering the silylation efficiency, approximately 24% of the silanol groups of material **3b** remained unsilylated, which is

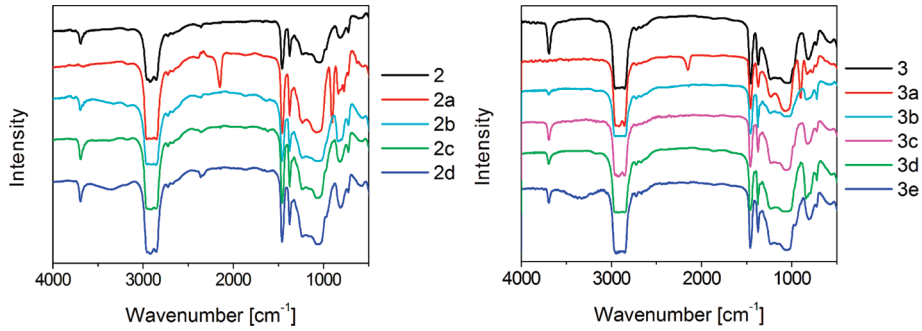

Figure 6. Infrared spectra of the surface-silylated SBA-1 materials under study: left, maximum $^1/_3$ of the SBA-1 silanol groups silylated; right, excess of silylating reagent has been used.

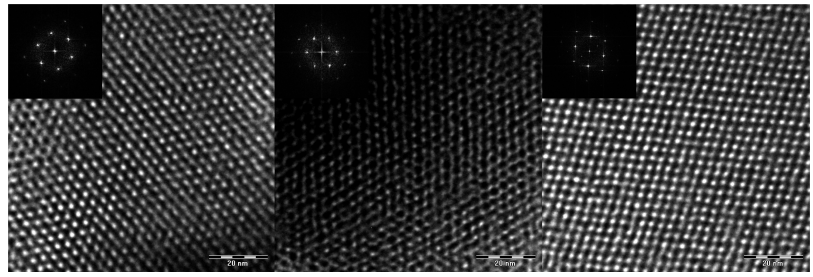

Figure 7. TEM images of SBA-1 materials **2** (left), **2b** (middle), and **3b** (right) from the [111] direction.

also supported by FTIR spectroscopy (Figure 6). According to the nitrogen physisorption measurement, significant BET surface area (30 m^2/g) and pore volume of material **3b** (0.01 cm^3/g) are no longer detectable, suggesting that the nitrogen molecules can no longer access the cages (kinetic diameter of $N_2 = 0.35$ nm). This effect is unique for the monosilazane (**A**)-treated SBA-1 and is not observed for the silylating reagents **B** and **C** (vide infra), even though a larger excess was used. Noteworthy, gaseous dimethylamine, the only coproduct of the monosilazane surface reaction, seems to be trapped inside the cages as evidenced by a considerable nitrogen content of the as-synthesized samples. For example, upon thermal treatment at 100 °C the nitrogen content of material **3b** dropped from 1.4% to below 0.1%. Chlorosilane **B** (regardless whether using a base or not) and ethoxysilane **C** are far less reactive and therefore lead to a more random distribution of the silyl groups over materials **3c**−**3e**. This can be explicitly seen from hybrid material **3d**: a relatively high carbon loading and hence a SE of 62% does not lead to pore blockage and the pore volume, derived from the *type I* isotherm, was found as 0.21 g/cm.[2] Kim et al. used differently sized chlorosilanes to identify the pore mouth diameter of different SBA-16 silicas[57] and Kruk et al.[91] stated that a C_8-ligand blocks pore openings up to 2.4 nm. The pore blockage observed for material **3b** therefore indicates that the size of the pore entrances of SBA-1 materials **2** and **3** are in the range of 15 × 22 Å, as determined by electron diffraction by Sakamoto et al.[88] TEM images of the monosilazane modified SBA-1 indicate preservation of the topology (Figure 7).

Silylation with ethoxysilane **C** gave a higher SE than with chlorosilane **B** (32% versus 19%; in the absence of NEt_3) even though a 1.5 fold excess of the silylation reagents was employed. All of the SBA-1 materials under study exhibit residual silanol groups as evidenced by the IR stretching vibration at 3695 cm^{-1} (Figure 6).

Conclusions

Monosilazane reagents of type Me_2NSiMe_2R display a higher silylation efficiency than similarly sized chloro- and alkoxysilanes as evidenced for the surface silylation of a MCM-41 silica with 4.0 nm pore diameter. The superior silylation behavior in such channel-like pore systems is rather kinetically controlled through the formation of the (sterically demanding) intermediate surface species than diffusion of the silylation reagents through the mesopores. For cagelike material SBA-1, monosilazane silylation is governed by the size-limiting effect of the cage windows. Whereas excess of the bulky reagent $Me_2NSiMe_2(C_8H_{17})$ leads to complete pore blockage, substoichiometric amounts of the same reagent can be exploited to tune the accessibility of the interior cages, because the rapid silylation occurs preferentially at the outer surface and at the pore openings. Such site-specific silylation can be exploited for size-selective catalytic transformations. Of course the size of the silyl substituent R plays an important role and has to be adjusted to the corresponding window size of the material. The less reactive chloro- and alkoxysilanes produce channel- and cagelike hybrid materials with a rather uniform and random distribution of silyl and hence remaining silanol groups. This reactivity behavior can be utilized for controlling the overall hydrophobicity of the surface as well as the amount and spacing of any (catalytically) active surface sites. It is clear from this silylation study that the various silylating reagents uniquely complement each other and that the choice of a silylating reagent should be driven by the application envisaged. For example, an effective synergism of tailor-made silazane reagents with cagelike mesoporous materials like SBA-1 can launch size-selective catalysts where the catalytic reaction is suggested to take place inside the meso-sized cages.

Acknowledgment. This research was supported by the NANOSCIENCE program of the Universitetet i Bergen.

Supporting Information Available: Detailed synthesis procedures; Figures of PXRD patterns of materials **1**, **2**, **3**, **4**, and **5**; nitrogen physisorption isotherms of materials **4a**−**d**; **5a**−**g**; IR spectra of materials **4a**−**d**; DRIFT spectra of materials **5a**−**g**; SEM images of materials **2a**, **2b**, **3b**, **5**, **5b**, and **5c**; and

TEM images of materials **5**, **5b**, and **5c**. This material is available free of charge via the Internet at http://pubs.acs.org.

References and Notes

(1) *Characterization and Chemical Modification of the Silica Surface*; Vansant, E. F., Van Der Voort, P., Vrancken, K. C., Eds. (University of Antwerp, Belgium); Elsevier: The Netherlands, 1995.

(2) Chen, J.; Li, Q.; Xu, R.; Xiao, F. *Angew. Chem., Int. Ed. Engl.* **1996**, *34*, 2694.

(3) Sutra, P.; Brunel, D. *Chem. Commun.* **1996**, 2485.

(4) Díaz, J. F.; Balkus, K. J., Jr.; Bedioui, F.; Kurshev, V.; Kevan, L. *Chem. Mater.* **1997**, *9*, 61.

(5) Lim, M. H.; Stein, A. *Chem. Mater.* **1999**, *11*, 3285.

(6) Anwander, R. *Chem. Mater.* **2001**, *13*, 4419.

(7) Marx, S.; Avnir, D. *Acc. Chem. Res.* **2007**, *40*, 768.

(8) Kresge, C. T.; Leonowicz, M. E.; Roth, W. J.; Vartuli, J. C.; Beck, J. S. *Nature* **1992**, *359*, 710.

(9) Huo, Q.; Leon, R.; Petroff, P. M.; Stucky, G. D. *Science* **1995**, *268*, 1324.

(10) Huo, Q.; Margolese, D. I.; Stucky, G. D. *Chem. Mater.* **1996**, *8*, 1147.

(11) Zhao, D.; Feng, J.; Huo, Q.; Melosh, N.; Fredrickson, G. H.; Chmelka, B. F.; Stucky, G. D. *Science* **1998**, *279*, 548.

(12) Zhao, D.; Huo, Q.; Feng, J.; Chmelka, B. F.; Stucky, G. D. *J. Am. Chem. Soc.* **1998**, *120*, 6024.

(13) Kleitz, F.; Liu, D.; Anilkumar, G. M.; Park, I.-S.; Solovyov, L. A.; Shmakov, A. N.; Ryoo, R. *J. Phys. Chem. B* **2003**, *107*, 14296.

(14) Zhao, X. S.; Lu, G. Q. *J. Phys. Chem. B* **1998**, *102*, 1556.

(15) Kim, S.; Ida, J.; Guliants, V. V.; Lin, J. Y. S. *J. Phys. Chem. B* **2005**, *109*, 6287.

(16) Donnet, J.-B.; Ridaoui, H.; Balard, H.; Barthel, H.; Gottschalk-Gaudig, T. *J. Colloid Interface Sci.* **2008**, *325*, 101.

(17) Raimondo, M.; Perez, G.; Sinibaldi, M.; De Stefanis, A.; Tomlinson, A. A. G. *Chem. Commun.* **1997**, 1343.

(18) Moller, K.; Bein, T. *Chem. Mater.* **1998**, *10*, 2950.

(19) Ozin, G. A.; Kuperman, A.; Stein, A. *Angew. Chem.* **1989**, *101*, 373.

(20) Komarneni, S.; Pidugu, R.; Menon, V. C. *J. Porous Mater.* **1996**, *3*, 99.

(21) Fan, H.; Lu, Y.; Stump, A.; Reed, S. T.; Baer, T.; Schunk, R.; Perez-Luna, V.; López, G. P.; Brinker, C. J. *Nature* **2000**, *405*, 56.

(22) Anwander, R. *Top. Curr. Chem.* **1996**, *179*, 33.

(23) Anwander, R.; Palm, C. *Stud. Surf. Sci. Catal.* **1998**, *117*, 413.

(24) Anwander, R.; Palm, C.; Stelzer, J.; Groeger, O.; Engelhardt, G. *Stud. Surf. Sci. Catal.* **1998**, *117*, 135.

(25) Kantam, M. L.; Bandyopadhyay, T.; Rahman, A.; Reddy, N. M.; Choudary, B. M. *J. Mol. Catal. A: Chem.* **1998**, *133*, 293.

(26) Mal, N. K.; Fujiwara, M.; Tanaka, Y. *Nature* **2003**, *421*, 350.

(27) Kidder, M. K.; Britt, P. F.; Zhang, Z.; Dai, S.; Hagaman, E. W.; Chaffee, A. L.; Buchanan, A. C., III *J. Am. Chem. Soc.* **2005**, *127*, 6353.

(28) Hoffmann, F.; Cornelius, M.; Morell, J.; Fröba, M. *Angew. Chem., Int. Ed.* **2006**, *45*, 3216.

(29) Cheng, K.; Landry, C. C. *J. Am. Chem. Soc.* **2007**, *129*, 9674.

(30) Zapilko, C.; Liang, Y.; Nerdal, W.; Anwander, R. *Chem.—Eur. J.* **2007**, *13*, 3169.

(31) D'Amore, M. B.; Schwarz, S. *Chem. Commun.* **1999**, 121.

(32) Mal, N. K.; Fujiwara, M.; Tanaka, Y.; Taguchi, T.; Matsukata, M. *Chem. Mater.* **2003**, *15*, 3385.

(33) Burkett, S. L.; Sims, S. D.; Mann, S. *Chem. Commun.* **1996**, 1367.

(34) Hall, S. R.; Fowler, C. E.; Lebeau, B.; Mann, S. *Chem. Commun.* **1999**, 201.

(35) Macquarrie, D. J. *Chem. Commun.* **1996**, 1961.

(36) Lim, M. H.; Blanford, C. F.; Stein, A. *J. Am. Chem. Soc.* **1997**, *119*, 4090.

(37) Richer, R.; Mercier, L. *Chem. Commun.* **1998**, 1775.

(38) Richer, R.; Mercier, L. *Chem. Mater.* **2001**, *13*, 2999.

(39) Huh, S.; Wiench, J. W.; Yoo, J.-C.; Pruski, M.; Lin, V. S.-Y. *Chem. Mater.* **2003**, *15*, 4247.

(40) Mercier, L.; Pinnavaia, T. J. *Adv. Mater.* **1997**, *9*, 500.

(41) Asefa, T.; Kruk, M.; MacLachlan, M. J.; Coombs, N.; Grondey, H.; Jaroniec, M.; Ozin, G. A. *J. Am. Chem. Soc.* **2001**, *123*, 8520.

(42) Burleigh, M. C.; Markowitz, M. A.; Spector, M. S.; Gaber, B. P. *Chem. Mater.* **2001**, *13*, 4760.

(43) Burleigh, M. C.; Jayasundera, S.; Spector, M. S.; Thomas, C. W.; Markowitz, M. A.; Gaber, B. P. *Chem. Mater.* **2004**, *16*, 3.

(44) Xia, Y.; Wang, W.; Mokaya, R. *J. Am. Chem. Soc.* **2005**, *127*, 790.

(45) Alauzun, J.; Mehdi, A.; Reyé, C.; Corriu, R. J. P. *J. Am. Chem. Soc.* **2006**, *128*, 8718.

(46) Capel-Sanchez, M. C.; Barrio, L.; Campos-Martin, J. M.; Fierro, J. L. G. *J. Colloid Interface Sci.* **2004**, *277*, 146.

(47) Anwander, R.; Nagl, I.; Widenmeyer, M.; Engelhardt, G.; Groeger, O.; Palm, C.; Röser, T. *J. Phys. Chem. B* **2000**, *104*, 3532.

(48) Tatsumi, T.; Koyano, K. A.; Tanaka, Y.; Nakata, S. *Stud. Surf. Sci. Catal.* **1998**, *117*, 143.

(49) Koyano, K. A.; Tatsumi, T.; Tanaka, Y.; Nakata, S. *J. Phys. Chem. B* **1997**, *101*, 9436.

(50) Matsumoto, A.; Tsutsumi, K.; Schumacher, K.; Unger, K. K. *Langmuir* **2002**, *18*, 4014.

(51) Jaroniec, C. P.; Kruk, M.; Jaroniec, M.; Sayari, A. *J. Phys. Chem. B* **1998**, *102*, 5503.

(52) Park, M.; Komarneni, S. *Microporous Mesoporous Mater.* **1998**, *25*, 75.

(53) Antochshuk, V.; Jaroniec, M. *J. Phys. Chem. B* **1999**, *103*, 6252.

(54) Antochshuk, V.; Jaroniec, M. *Chem. Commun.* **1999**, 2373.

(55) Antochshuk, V.; Jaroniec, M. *Chem. Mater.* **2000**, *12*, 2496.

(56) De Juan, F.; Ruiz-Hitzky, E. *Adv. Mater.* **2000**, *12*, 430.

(57) Kim, T.-W.; Ryoo, R.; Kruk, M.; Gierszal, K. P.; Jaroniec, M.; Kamiya, S.; Terasaki, O. *J. Phys. Chem. B* **2004**, *108*, 11480.

(58) Liu, Y.-H.; Lin, H.-P.; Mou, C.-Y. *Langmuir* **2004**, *20*, 3231.

(59) Brandhuber, D.; Huesing, N.; Raab, C. K.; Torma, V.; Peterlik, H. *J. Mater. Chem.* **2005**, *15*, 1801.

(60) Brandhuber, D.; Peterlik, H.; Huesing, N. *J. Mater. Chem.* **2005**, *15*, 3896.

(61) Zapilko, C.; Widenmeyer, M.; Nagl, I.; Estler, F.; Anwander, R.; Raudaschl-Sieber, G.; Groeger, O.; Engelhardt, G. *J. Am. Chem. Soc.* **2006**, *128*, 16266.

(62) Choplin, A. *J. Mol. Catal.* **1994**, *86*, 501.

(63) Fowler, C. E.; Burkett, S. L.; Mann, S. *Chem. Commun.* **1997**, 1769.

(64) Richer, R.; Mercier, L. *Chem. Commun.* **1998**, 1775.

(65) Bellocq, N.; Abramson, S.; Laspéras, M.; Brunel, D.; Moreau, P. *Tetrahedron: Asymmetry* **1999**, *10*, 3229.

(66) Lin, H.-P.; Yang, L.-Y.; Mou, C.-Y.; Liu, S.-B.; Lee, H.-K. *New J. Chem.* **2000**, *24*, 253.

(67) Zapilko, C.; Anwander, R. *Chem. Mater.* **2006**, *18*, 1479.

(68) Haukka, S.; Root, A. *J. Phys. Chem.* **1994**, *98*, 1695.

(69) Derrien, A.; Renard, G.; Brunel, D. *Stud. Surf. Sci. Catal.* **1998**, *117*, 445.

(70) Wright, J. M.; Jones, G. B. *Tetrahedron Lett.* **1999**, *40*, 7605.

(71) Gerstberger, G.; Anwander, R. *Microporous Mesoporous Mater.* **2001**, *44−45*, 303.

(72) Zapilko, C.; Liang, Y.; Anwander, R. *Chem. Mater.* **2007**, *19*, 3171.

(73) Hertl, W.; Hair, M. L. *J. Phys. Chem.* **1971**, *75*, 2181.

(74) Shimada, T.; Aoki, K.; Shinoda, Y.; Nakamura, T.; Tokunaga, N.; Inagaki, S.; Hayashi, T. *J. Am. Chem. Soc.* **2003**, *125*, 4688.

(75) Dai, L.-X.; Teng, Y.-H.; Tabata, K.; Suzuki, E.; Tatsumi, T. *Microporous Mesoporous Mater.* **2001**, *44−45*, 573.

(76) Hunter, H. M. A.; Wright, P. A. *Microporous Mesoporous Mater.* **2001**, *43*, 361.

(77) Morey, M. S.; Davidson, A.; Stucky, G. D. *J. Porous Mater.* **1998**, *5*, 195.

(78) Schnitzlbaumer, M. Rare-Earth Metal Alkoxides on Periodic Mesoporous Silica, Ph.D. Thesis, Technische Universität München, Munich, Germany, 2006.

(79) Widenmeyer, M. Periodic Mesoporous Silica: Synthesis and Surface Functionalization, Ph.D. Thesis, Technische Universität München, Munich, Germany, 2001.

(80) Kim, M. J.; Ryoo, R. *Chem. Mater.* **1999**, *11*, 487.

(81) Brunauer, S.; Emmett, P. H.; Teller, E. *J. Am. Chem. Soc.* **1938**, *60*, 309.

(82) Sing, K. S. W.; Everett, D. H.; Haul, R. A. W.; Moscou, L.; Pierotti, R. A.; Roquérol, J.; Siemieniewska, T. *Pure Appl. Chem.* **1985**, *57*, 603.

(83) Barrett, E. P.; Joyner, L. G.; Halenda, P. P. *J. Am. Chem. Soc.* **1951**, *73*, 373.

(84) Ravikovitch, P. I.; Neimark, A. V. *Langmuir* **2002**, *18*, 1550.

(85) Sayari, A.; Liu, P.; Kruk, M.; Jaroniec, M. *Chem. Mater.* **1997**, *9*, 2499.

(86) Kruk, M.; Antochshuk, V.; Jaroniec, M.; Sayari, A. *J. Phys. Chem. B* **1999**, *103*, 10670.

(87) Vinu, A.; Murugesan, V.; Hartmann, M. *Chem. Mater.* **2003**, *15*, 1385.

(88) Sakamoto, Y.; Kaneda, M.; Terasaki, O.; Zhao, D. Y.; Kim, J. M.; Stucky, G.; Shin, H. J.; Ryoo, R. *Nature* **2000**, *408*, 449.

(89) Anderson, M. W.; Egger, C. C.; Tiddy, G. J. T.; Casci, J. L.; Brakke, K. A. *Angew. Chem., Int. Ed.* **2005**, *44*, 3243.

(90) Yoshida, W.; Castro, R. P.; Jou, J.-D.; Cohen, Y. *Langmuir* **2001**, *17*, 5882.

(91) Kruk, M.; Antochshuk, V.; Matos, J. R.; Mercuri, L. P.; Jaroniec, M. *J. Am. Chem. Soc.* **2002**, *124*, 768.

JP107749G